Inorganic Chemistry

Article

pubs.acs.org/IC

Copper Coordination to Native N-Terminally Modified versus Full-Length Amyloid-β: Second-Sphere Effects Determine the Species Present at Physiological pH

Bruno Alies,*[,†,‡] Christian Bijani,[†,‡] Stéphanie Sayen,[§] Emmanuel Guillon,[§] Peter Faller,[†,‡] and Christelle Hureau*[,†,‡]

[†]Laboratoire de Chimie de Coordination (LCC), CNRS, 205 route de Narbonne, F-31077 Toulouse, France

[‡]UPS, INPT, LCC, Université de Toulouse, F-31077 Toulouse, France

[§]Groupe de Chimie de Coordination, Institut de Chimie Moléculaire de Reims (ICMR, CNRS UMR 7312), Université de Reims Champagne-Ardenne, BP 1039, 51687 Reims Cedex 2, France

Supporting Information

ABSTRACT: Alzheimer's disease is characterized by senile plaques in which metallic ions (copper, zinc, and iron) are colocalized with amyloid-β peptides of different sequences in aggregated forms. In addition to the full-length peptides (Aβ1-40/42), N-terminally truncated Aβ3-40/42 forms and their pyroglutamate counterparts, Aβp3-40/42, have been proposed to play key features in the aggregation process, leading to the senile plaques. Furthermore, they have been shown to be more toxic than the full-length Aβ, which made them central targets for therapeutic approaches. In order to better disentangle the possible role of metallic ions in the aggregation process, copper(II) coordination to the full-length amyloid peptides has been extensively studied in the last years. However, regarding the N-terminally modified forms at position 3, very little is known. Therefore, copper(I) and copper(II) coordination to those peptides have been investigated in the present report using a variety of complementary techniques and as a function of pH. Copper(I) coordination is not affected by the N-terminal modifications. In contrast, copper(II) coordination is different from that previously reported for the full-length peptide. In the case of the pyroglutamate form, this is due to preclusion of N-terminal amine binding. In the case of the N-terminally truncated form, alteration in copper(II) coordination is caused by second-sphere effects that impact the first binding shell and the pH-dependent repartition of the various [Cu(peptide)] complexes. Such second-sphere effects are anticipated to apply to a variety of metal ions and peptides, and their importance on changing the first binding shell has not been fully recognized yet.

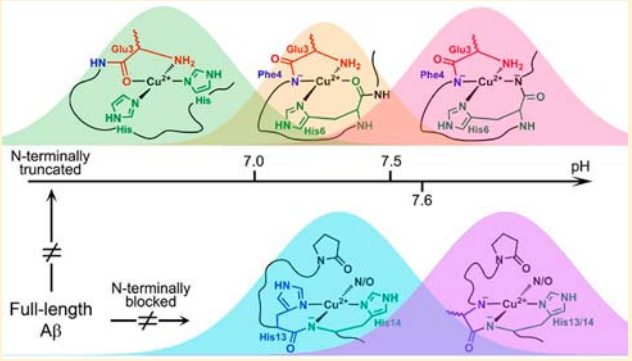

INTRODUCTION

Amyloid-β (Aβ) is mainly a 40/42 amino acid residue peptide that is normally present under physiological conditions, especially in the brain. Despite a wide number of studies, its biological function is still under debate.[1] Aβ is well-known to be the main component of senile plaque, a typical feature that occurs in the brain of Alzheimer's disease (AD) patients.[2] According to the amyloid cascade hypothesis, aggregation of the monomeric Aβ into the fibrils detected in the senile plaque plays a causal role in AD.[3] The amyloid cascade contains several aggregation stages (oligomers, protofibrils, and fibrils), and aggregation intermediates (often called oligomers) have been proposed to instigate further pathological events, including the formation of intracellular neurofibrillary tangles, another hallmark of AD, and disruption of synaptic connections, which would lead ultimately to neuronal cell death and dementia.[3−5] They are now considered to be more toxic than the senile plaques or higher molecular weight aggregates,[5−7] via various events including the production of reactive oxygen species (ROS), which have also been implicated in the pathological process. Metal ions such as copper, iron, and zinc are found at hundreds of micromolars in senile plaques.[8,9] Their effects on Aβ aggregation and their involvement in the generation of ROS, two key features in the amyloid cascade, underline an important role of metallic ions in AD.[10−12]

In order to gain insight into the role of metallic ions in AD, coordination of copper to Aβ1-40/42 has been widely studied. It was shown that copper(II)[13−15] and copper(I)[16] bind to the first 16 amino acid residues and, hence, the C-terminally truncated Aβ1-16 peptide is widely accepted as a valuable model of copper binding to monomeric Aβ1-40/42. Copper-(II) binds Aβ with an apparent K_d in the low nanomolar range (at pH 7.4),[17−19] and copper coordination is pH-dependent.

Received: September 27, 2012
Published: November 14, 2012

   dx.doi.org/10.1021/ic302097d | *Inorg. Chem.* 2012, 51, 12988−13000

Near physiological pH, [Cu^{II}(Aβ)] species are found under two kinds of coordination modes (called "components" I and II),[20,21] in which the copper(II) geometry is square-planar. Components I and II have been characterized using electron paramagnetic resonance (EPR), including studies on copper(II) binding to specifically labelled Aβ peptides,[22−24] circular dichroism (CD),[25] and nuclear magnetic resonance (NMR).[15,26] The four copper(II) equatorial ligands in component I are NH_2 from the N-terminal Asp1, CO from the Asp1−Ala2 peptide bond, and two nitrogen atoms from the His rings of His6 and His13 or His14, with the latter two being in dynamical exchange for the fourth copper(II) equatorial position. In component II, the four ligands are the NH_2 terminal amine that remains coordinated, the deprotoned N^- amide group from the Asp1−Ala2 bond that replaces the corresponding CO group, the adjacent CO group from the Ala2−Glu3 peptide bond, and a side chain from one His (His6, His13, or His14 in dynamical exchange).

Recently, the species obtained at higher pH, i.e., components III and IV, have been characterized as well.[27] Component III equatorial ligands consist of $-NH_2$ (Asp1), two adjacent deprotonated amides N^- (from Asp1−Ala2 and Ala2−Glu3 peptide bonds), and one His. Component IV involves the N-terminal NH_2 (Asp1) and three adjacent deprotonated amides N^- (from Asp1−Ala2, Ala2−Glu3, and Glu3−Phe4 peptide bonds). Hence, the Roman numbers refer to the number of deprotonated amide function(s) involved in copper(II) binding (from I to IV for components involving from 0 to 3 deprotonated amide functions).

Regarding copper(I) coordination to the monomeric Aβ peptide, a consensual proposition has recently emerged in the literature: the copper(I) center is linearly bound by two side chains of His residues,[16,28] with equilibrium between the three possible pairs of His, His6−His13, His6−His14, and His13−His14, with the latter one being proposed as the predominant species.[29,30]

Aβ1-40/42 and familial mutants are not the only forms of interest. N-terminally modified peptides such as the Aβ3-40/42 truncated forms, the sequence of which begins by glutamate 3, and the pyroglumate Aβp3-40/42 counterpart have been found in AD brains in high amount (up to 25% of Aβ in plaques are pyroglutamate forms[31,32]) and have been extensively studied in the last years for several reasons. First, they have been shown to be more toxic than the full-length Aβ1-40/42,[33−37] possibly via modification of the amyloid plaque morphology.[38] Second, the N-term cyclization in Aβp3-40/42 slows down peptide degradation.[39] Third, the aggregation process of Aβ1-40/42 could change because of seeding effects of the pyroglutamate forms.[40−42]

Considering the role of copper ions in Aβ aggregation and ROS production processes linked to AD, it seems interesting to investigate the coordination chemistry of copper(I) and copper(II) to those N-terminally modified forms Aβ3-40/42 and Aβp3-40/42. So far, only one EPR study on the coordination chemistry copper(II) binding to models of Aβ3-40/42 and Aβp3-40/42, i.e., Aβ3-16 and Aβp3-16, was published.[43] On the basis of similar EPR parameters determined for the two [Cu^{II}(Aβ3-16)] and [Cu^{II}(Aβp3-16)] species, the authors suggested that copper(II) coordination to the Aβ3-16 and Aβp3-16 peptides are similar but with different pH dependence regarding the repartition of components I and II. As in [Cu^{II}(Aβp3-16)], copper(II) coordination via the terminal amine is precluded by the pyroglutamate ring; they thus proposed that the N-terminal amine is not directly involved in copper(II) binding in the [Cu^{II}(Aβ3-16)] complexes either. This result seems highly questionable because it has been shown in many studies and on several different Aβ peptide sequences that when the N-terminal amine is available, it takes part of the coordination sphere of copper(II) regardless of the pH values.[25,27]

In order to get a better description of copper(II) coordination to Aβ3-16 and Aβp3-16 peptides and possibly to disentangle the role of the $-NH_2$ terminus in copper(II) binding in such Aβ-modified forms, we have used EPR but also extended the analysis with complementary methods, i.e., ^{13}C NMR, CD, and X-ray absorption near-edge structure (XANES). In addition to these new pieces of data on copper(II), we have determined copper(I) coordination by ^1H NMR, and to complete the study, we have evaluated the copper(II) and copper(I) affinity for both N-terminally modified peptides. This complete set of analyses provided the first results on copper(I) and new insights into the coordination of copper(II) to such N-terminally modified peptides.

EXPERIMENTAL SECTION

Copper Solutions. Copper(II) used was from $CuSO_4{\cdot}5H_2O$ and purchased from Sigma. A stock solution of copper(II) (∼1 M) was prepared in D_2O. [$Cu^I(MeCN)_4$](BF_4) (MeCN = methyl cyanide) was bought from Sigma-Aldrich and kept under an inert atmosphere until use. A copper(I) stock solution (0.16 M) was prepared in MeCN.

Ferrozine [5,6-diphenyl-3-(2-pyridyl)-1,2,4-triazine-4,4″-disulfonic acid monosodium salt hydrate] was bought from Alfa-Aesar. A 0.1 M stock solution was prepared in water.

HEPES buffer (sodium salt of 2-[4-(2-hydroxyethyl)piperazin-1-yl]ethanesulfonic acid) was bought from Fluka (bioluminescence grade).

A phosphate buffer was prepared from K_2HPO_4 and KH_2PO_4 bought from Sigma-Aldrich.

Peptides. Aβ1-16 peptide (sequence DAEFRHDSGYEVHHQK), Ac-Aβ peptide corresponding to the N-terminally acetylated Aβ1-16 peptide, Aβ3-16 (sequence EFRHDSGYEVHHQK), and Aβp3-16 corresponding to the N-terminally pyroglumate form of the Aβ3-16 peptide (sequence pEFRHDSGYEVHHQK) were bought from GeneCust (Dudelange, Luxembourg) with purity grade >98%.

Cu(peptide) Sample Preparation. Studies were performed in H_2O or D_2O. However, for clarity and consistency, we decided to use the notation pH even when the measurements were made in D_2O. The pD was measured using a classical glass electrode according to pD = pH* + 0.4, and the apparent pH value was adjusted according to ref 44, pH = (pD − 0.32)/1.044, or equivalently to ref 45, pH = 0.929pH* + 0.41, to be in ionization conditions equivalent to those in H_2O.

Stock solutions of peptide were prepared by dissolving the powder in Milli-Q water or D_2O (resulting pH ∼ 2). The peptide concentration was then determined by UV−vis absorption of Tyr10 considered as free tyrosine ($\varepsilon_{276} - \varepsilon_{296}$ = 1410 M^{-1} cm^{-1}), and the solution was diluted to the appropriate concentration in peptide. The pH was adjusted using NaOH/HCl (H_2O) or NaOD/DCl (D_2O). All pH values are given with a ±0.2 pH unit error.

Circular Dichroism (CD) Samples. A stock solution of peptide was diluted to 0.5 mM in pure Milli-Q water. A total of 0.9 equiv of Cu^{II} was added from a 0.1 M $Cu(SO_4)$ stock solution.

Electron Paramagnetic Resonance (EPR) Samples. A stock solution of peptide was diluted to 1.0 mM in D_2O. A total of 0.9 equiv of $^{63}Cu^{II}$ was added from a 0.1 M $^{63}Cu(NO_3)_2$ stock solution. Samples were frozen in quartz tubes after the addition of 10% glycerol as a cryoprotectant.

Nuclear Magnetic Resonance (NMR) Samples. For NMR copper(II) experiments, a stock solution of Aβ3-16 or Aβp3-16 peptide was diluted to about 10 mM in D_2O. A substoichiometric

dx.doi.org/10.1021/ic302097d | Inorg. Chem. 2012, 51, 12988−13000

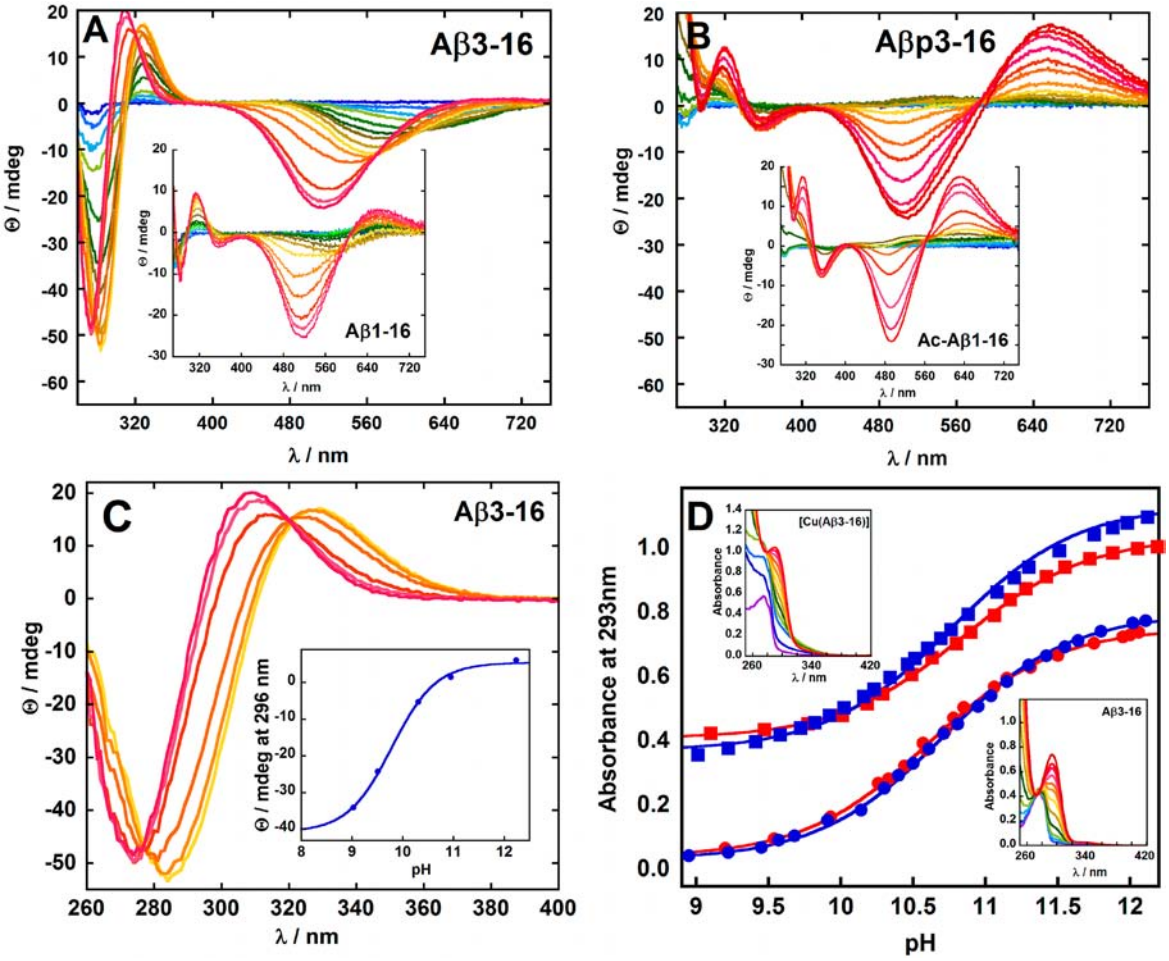

Figure 1. pH dependence of copper(II) coordination to Aβ3-16 (panel A) and Aβ1-16 (inset in panel A) and to Aβp3-16 (panel B) and Ac-Aβ1-16 (insert in panel B) from acidic (blue) to basic (red) pH values. Panel C: Zoom on the UV band of [Cu(Aβ3-16)] between pH 9 and 12 and pH dependence of the UV band at 296 nm detected by CD (inset in panel C). Panel D: pH dependence of the UV band at 293 nm detected by UV−vis for Aβ1-16 (blue) and Aβ3-16 (red) peptides and of the corresponding copper(II) complexes. Insets in panel D are the UV−vis spectrum of Aβ3-16 and [Cu(Aβ3-16)]. [Cu^{II}(peptide)] = 0.45 mM (panels A−C), [Cu^{II}(peptide)] = 0.3 mM (panel D), and l = 1 cm.

quantity (ca. 0.02 equiv at pH 6 or 0.3 equiv at pH 8.6 for the Aβ3-16 peptide and 0.05 equiv at pH 7 for the for the Aβp3-16 peptide) of copper(II) from $Cu(SO_4)$ in D_2O was added. Indeed, a too high copper(II)-to-Aβ ratio would induce an uncontrolled broadening of NMR signals because of paramagnetism of the copper(II). Nevertheless, this ratio needs to be enough to induce selective broadening of specific residues of all of the peptides present in solution [via exchange of copper(II) between peptides].

For NMR copper(I) experiments, copper(I) was produced in situ, by the direct addition (1.5 equiv) of a fresh-made $Na_2S_2O_3$ stock solution (0.1 M) into an NMR tube previously degassed with water-saturated argon containing the peptides and copper(II), both at 1 mM concentration. The NMR tube was sealed under argon, measured as soon as possible to prevent possible oxidation. In such conditions, no significant pH drift due to the addition of $Na_2S_2O_3$ was measured.

UV−Vis Samples. For ferrozine titration experiments, copper(I) stock solutions (5 mM) were prepared in an argon-degassed HEPES buffer [0.1 M, pH 7.4, containing 5% (v/v) MeCN] and degassed with water-saturated argon just before use. UV−vis monitoring of the stock solution under argon was performed to ensure that under these conditions no dismutation occurred. Less than 2% of copper(II) was detected, a content that can be neglected in analysis of the titration curve.

CD. CD spectra were recorded at 20 °C on a Jasco J-815 CD spectrometer, with a Peltier PTC423 temperature controller. Data were collected with a 1 nm sampling interval, and two scans were averaged and a baseline spectrum was subtracted for each spectrum.

EPR. EPR data were recorded using an Elexsys E 500 Bruker spectrometer, operating at a microwave frequency of approximately 9.5 GHz. All spectra were recorded using a microwave power of 20 mW across a sweep width of 150 mT (centered at 310 mT) with a modulation amplitude of 0.5 mT. Experiments were carried out at 110 K using a liquid-nitrogen cryostat.

NMR. 1D ^1H and ^{13}C NMR experiments and 2D experiments were recorded on a Bruker Avance 500 spectrometer equipped with a 5-mm triple-resonance inverse Z-gradient probe (TBI ^1H, ^{31}P, BB). All chemical shifts are relative to tetramethylsilane. 1D and 2D NMR spectra were collected at 298 K in pure D_2O, respectively. Accumulation lasted ca. 16 h for the $^{13}C\{^1H\}$ NMR experiments and 24 h for the 2D $^1H-^1H$ TOCSY, $^1H-^{13}C$ HSQC, and $^1H-^{13}C$ HMBC experiments.

All of the ^1H and ^{13}C NMR signals were assigned on the basis of chemical shifts, spin−spin coupling constants, splitting patterns, and signal intensities and by using $^1H-^1H$ TOCSY, $^1H-^{13}C$ HSQC, and $^1H-^{13}C$ HMBC experiments.

XANES. Measurements were carried out at the SOLEIL Synchrotron Facility (St. Aubin, France), which was operating with a ring current of 400 mA. Cu K-edge XANES spectra were collected on the SAMBA beamline using a Si(220) double crystal monochromator and two large silicon mirrors for high-energy harmonics rejection. The liquid samples were injected in special sample holders

dx.doi.org/10.1021/ic302097d | *Inorg. Chem.* 2012, 51, 12988−13000

and cooled down to 20−30 K using a helium-flow cryostat. The spectra were collected in fluorescence mode by measuring the Cu Kα fluorescence with a seven-element germanium detector (Canberra). Three scans of 25 min each were averaged. Data from each detector channel were inspected for glitches or dropouts before inclusion in the final average. Energy calibration was achieved by recording a copper foil for the Cu edge and assigning the first inflection point of the absorption spectrum to 8980.3 eV. XANES spectra were background-corrected by linear regression through the preedge region and a polynomial through the postedge region and normalized to the edge jump. No significant photoreduction of the samples occurs during the measurements.

RESULTS

Structural Data on [Cu(Aβ3-16)] and [Cu(Aβp3-16)]. *pH Dependence on the CD Study of [Cu^{II}(Aβ3-16)] and [Cu^{II}(Aβp3-16)].* CD is a powerful tool to sense structural changes due to metal-ion coordination to peptide. In the case of copper(II) complexes, the d−d and charge-transfer transitions can be studied between 450 to 750 nm and between 250 and 400 nm, respectively.[46] CD is thus sensitive to structural changes in the first copper(II) coordination sphere but also to modifications beyond the first shell.[47] pH-dependent CD spectra were recorded for the four [Cu^{II}(Aβ1-16)], [Cu^{II}(Aβ3-16)], [Cu^{II}(Ac-Aβ1-16)], and [Cu^{II}(Aβp3-16)] complexes (Figure 1A,B). All four studied complexes show different signatures, underlining different first and second coordination shells. Nevertheless, general trends can be observed. In all of the complexes, the intensity of the deprotonated amide-to-copper(II) ligand-to-metal charge-transfer (LMCT) transitions increases from pH ∼ 6, indicating participation of the deprotonated amide in copper(II) binding above this pH value. Furthermore, the d−d transition bands evolve from approximately 650 nm at low pH to 500 nm at high pH. This hypsochromic shift indicates a copper(II) environment that gets enriched in nitrogen atoms (compared to oxygen atoms) at higher pH, in line with successive amide backbone deprotonation and subsequent copper(II) binding with a pH increase. Another important feature is the strong similarity between [Cu^{II}(Aβ1-16)] and [Cu^{II}(Aβ3-16)] on the one side and [Cu^{II}(Ac-Aβ1-16)] and [Cu^{II}(Aβp3-16)] on the other side (compare parts A and B of Figure 1 and parameters listed in Table 1). Thus, two families can be made: [Cu^{II}(Aβ1-16)]-like families obtained when the peptide possesses a free $-NH_2$ terminus (Figure 1A) and [Cu^{II}(Ac-Aβ1-16)]-like families when the peptide has the $-NH_2$ terminus blocked (Figure 1B). Two clear spectral differences between the two families can be observed: (i) A negative band at ∼280 nm attributed to NH_2-to-copper(II) LMCT appears only in the former family. This indicates the involvement of the $-NH_2$ terminal amine in copper(II) binding regardless of the pH. Such a CD feature is not observed in the latter family in line with a $-NH_2$ terminal amine, which is blocked either via acetylation (Ac-Aβ1-16) or via pyroglutamate formation (Aβp3-16). (ii) On the [Cu^{II}(Ac-Aβ1-16)] and [Cu^{II}(Aβp3-16)] spectra, an intense positive CD band is observed at ∼645 nm, while on [Cu^{II}(Aβ1-16)] and [Cu^{II}(Aβ3-16)] spectra, such a band is not detected. These two main differences strongly suggest two highly different copper(II) sites between [Cu^{II}(Aβ1-16)] and [Cu^{II}(Aβ3-16)], on the one hand, and [Cu^{II}(Ac-Aβ1-16)] and [Cu^{II}(Aβp3-16)], on the other hand, regardless of the pH range. Such strong dissimilarities are reminiscent of first-coordination-shell effects. In a more thorough analysis, minor differences, indicative of second-

Table 1. EPR Parameters and CD Data of the Four Different [Cu(Aβ1-16)], [Cu(Aβ3-16)], [Cu(AcAβ1-16)], and [Cu(Aβp3-16)] Species as a Function of the pH and Corresponding pK_a Values[a]

	I				II				III				IV				pK_a				
	I′				II′				III′				IV′								
peptide	$g_{\|}^b$	$A_{\|}$ ($\times10^{-4}$ cm^{-1})	λ_{max} (nm)		$g_{\|}$	$A_{\|}$ ($\times10^{-4}$ cm^{-1})	λ_{max} (nm)		$g_{\|}$	$A_{\|}$ ($\times10^{-4}$ cm^{-1})	λ_{max} (nm)		$g_{\|}$	$A_{\|}$ ($\times10^{-4}$ cm^{-1})	λ_{max} (nm)		I/II	II/III	III/IV	ref^b
Aβ1-16	2.26(2)	184	660+		2.22(6)	161	580−		2.19(1)	194			2.17(3)	203	516−, 660+		7.8	9.3	10.1	27
Aβ3-16	2.25(4)	182	640−		2.22(3)	160	602−		2.19(0)	201	574−		2.16(7)	212	515−		7.0	7.5	10.0	this work
Aβ3-16	2.26(1)	183							2.19(4)	193										43
	I′				II′				III′				IV′				I′/II′	II′/III′	III′/IV′	
peptide	$g_{\|}^b$	$A_{\|}$ ($\times10^{-4}$ cm^{-1})	λ_{max} (nm)		$g_{\|}$	$A_{\|}$ ($\times10^{-4}$ cm^{-1})	λ_{max} (nm)		$g_{\|}$	$A_{\|}$ ($\times10^{-4}$ cm^{-1})	λ_{max} (nm)		$g_{\|}$	$A_{\|}$ ($\times10^{-4}$ cm^{-1})	λ_{max} (nm)		I/II	II/III	III/IV	ref
AcAβ 1-16	2.32(0)	168			2.27(3)	187	580+		2.23(0)	171	645+, 485−		2.19(1)	190	635+, 495−		5.2	7.5	8.7	27
Aβp3-16	2.31(0)	169			2.26(4)	180	560+		2.23(0)	161	656+, 500−		2.19(0)	187	657+, 510−		5.3	7.6	8.8	this work
Aβp3-16					2.26(1)	183							2.19(4)	193						43

[a]In the CD data, the ± sign indicates the positive/negative nature of the band. [b]Numbers into parentheses are the third digit of the $g_{\|}$ value, which is given with an error of ±0.005. In ref 27 and in this work, parallel spin Hamiltonian parameters were obtained directly from the experimental spectra and were calculated from the second and third hyperfine lines in order to remove second-order effects. Errors on the hyperfine couplings are ±5 × 10^{-4} cm^{-1} and on the pK_a values ±0.2.

dx.doi.org/10.1021/ic302097d | Inorg. Chem. 2012, 51, 12988−13000

sphere effects, are observed between the CD spectra of [Cu^{II}(Aβ1-16)] and [Cu^{II}(Aβ3-16)] complexes. For instance, d−d transitions are slightly different, with positive CD bands detected in the [Cu^{II}(Aβ1-16)] spectrum and only negative CD bands in the case of the [Cu^{II}(Aβ3-16)] complex. Also the two $-NH_2$-to-copper(II) and deprotonated amide-to-copper(II) LMCT bands are detected near 285 and 315 nm, respectively, in the case of the [Cu^{II}(Aβ1-16)] complex, while the same bands shift from 330 to 315 nm and from 285 to 275 nm with an increase of the pH (pK_a = 9.8; Figure 1C) in the case of the [Cu^{II}(Aβ3-16)] complex. This pK_a value is close to that expected for deprotonation of the Tyr10 residue, and thus to examine whether Tyr10 deprotonation is at the origin of such a band shift in the case of the Aβ3-16 peptide, UV−vis pH titration was performed for both peptides (Aβ1-16 and Aβ3-16) and corresponding copper(II) complexes (Figure 1D). Deprotonation of the Tyr residue is close between the apo- and holopeptide and between the two peptides (pK_a = 10.7 ± 0.1). Hence, the shift in the N^--to-copper(II) LMCT band observed near pH 9.8 only detected for the [Cu^{II}(Aβ3-16)] species is not linked to deprotonation of the Tyr residue, indicating a difference in the second-sphere environment between [Cu^{II}(Aβ3-16)] and [Cu^{II}(Aβ1-16)] that does not persist above pH 9.8. Indeed above this pH value, both complexes exhibit the same N^--to-copper(II) LMCT at 315 nm (Figure 1A,C). In addition, it appears that no Tyr10 coordination to copper(II) is observed either in the case of the [Cu^{II}(Aβ1-16)] complex, as previously reported,[15,24,25,48,49] or in the case of the [Cu^{II}(Aβ3-16)] complex, in line with the absence of tyrosinate-to-copper(II) LMCT transition detected near 400 nm.[50]

pH Dependence on the EPR Study of [Cu^{II}(Aβ3-16)] and [Cu^{II}(Aβp3-16)]. EPR has been widely used to gain insight into copper(II) coordination because different copper(II) environments and geometries lead to different EPR parameters.[46] In particular, EPR parameters are correlated to the number, chemical nature, and charge of the equatorial ligands.[51] The pH dependence of the EPR fingerprints of the four [Cu(Aβ1-16)], [Cu(Aβ3-16)], [Cu(Ac-Aβ3-16)], and [Cu(Aβp3-16)] complexes have been studied over a wide pH range (3−12; Figure S1 in the Supporting Information). This allowed determination of the speciation, i.e., the different types of coordination environments and their relative abundance as a function of the pH. With respect to the previous work,[27] the different components encountered in [Cu(Aβ1-16)] and [Cu(Aβ3-16)] (respectively [Cu(Ac-Aβ)] and [Cu(Aβp3-16)]) were denoted as I−IV (respectively I′−IV′). According to the two families observed by CD, we have regrouped in Figure 2A the EPR spectra of [Cu(Aβ1-16)] (black) and [Cu(Aβ3-16)] (gray) and in Figure 2B the EPR spectra of [Cu(Ac-Aβ1-16)] (black) and [Cu(Aβp3-16)] (gray), where the spectra are compared at some selected pH values. In Figure 2A, the two lower traces display the EPR signatures of the two components I (blue) and II (green) in a 1:1 ratio of [Cu(Aβ1-16)] (black, pH 7.8) and [Cu(Aβ3-16)] (gray, pH 7.0). The EPR signatures are very similar, in line with the same type of first-sphere copper(II) coordination in the two peptides for both components I and II. The EPR parameters (Table 1) of components I and II are consistent with a 3N1O coordination mode, as previously discussed in the case of the Aβ1-16 peptide.[13,17,21,25] The middle trace [Cu(Aβ3-16)] (yellow, pH 8.7) is attributed to component III, a component that is hardly detected in the case of [Cu(Aβ1-16)][27] because of the

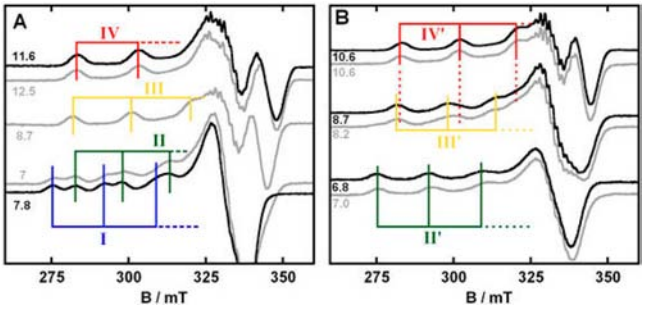

Figure 2. EPR spectra of copper(II) peptide complexes at selected pH values. Panel A: [Cu(Aβ1-16)] (black); [Cu(Aβ3-16)] (gray). Panel B: [Cu(AcAβ1-16)] (black); [Cu(Aβp3-16)] (gray). [Cu(peptide)] = 0.9 mM in D_2O, ν = 9.5 GHz, amplitude modulation = 0.5 mT, microwave power = 20 mW, and T = 110 K.

simultaneous presence of components II and IV. The two upper traces [Cu(Aβ1-16)] (black, pH 11.6) and [Cu(Aβ3-16)] (gray, pH 12.5) show the signature of component IV (red) of both complexes. EPR parameters of components III and IV are consistent with a 4N coordination sphere. In Figure 2B, EPR spectra of [Cu(Ac-Aβ3-16)] (black) and [Cu(Aβp3-16)] (gray) are compared at different pH values. The two complexes display the same EPR signatures at similar pH values. Three different components are observed. The high similarities between the EPR fingerprints of [Cu(Ac-Aβ3-16)] and [Cu(Aβp3-16)] suggest that the coordination of copper(II) will be similar in both peptides whatever the pH. Hence, the four components observed from pH 5 are denoted as I′−IV′, corresponding to complexes with 0 to 3 deprotonated amides bound to copper(II), with respect to previous work.[27] Together with the EPR parameters, the pK_a values between two successive components are reported in Table 1. From these pK_a values, it is possible to evaluate the relative proportion of the different components at a given pH. For the physiological pH 7.4, in the case of [Cu(Aβ1-16)] having a pK_a(I/II) = 7.8,[27] the major component is I with a weak contribution of component II. In contrast, for [Cu(Aβ3-16)] with a pK_a(I/II) = 7.0 [evaluated from the 50:50 proportion of components I and II at pH 7.0 (Figure 2A)] and a pK_a(II/III) = 7.5 [evaluated from the 50:50 proportion of components II and III (Figure S2 in the Supporting Information)], the main component is II with a significant contribution of component III. Consequently, the type of copper(II) coordination at physiological pH is significantly different between the two peptides. For [Cu(Aβp3-16)] species with pK_a(II′/III′) = 7.6 [evaluated from the 50:50 proportion of components II′ and III′ (Figure S2 in the Supporting Information)], II′ is the major component at pH 7.4 with a large contribution of component III′, as is also the case for the [Cu(Ac-Aβ1-16)] complex. This underlines the fact that, for those two latter species, the EPR parameters *and* pH dependence are highly similar, indicating, as expected, that the influence of how the N-term is modified (actelyation or pyroglutamate formation) is weak regarding Cu(II) coordination.

^{13}C NMR Study of [Cu^{II}(Aβ3-16)] and [Cu^{II}(Aβp3-16)]. In order to identify ligands involved in copper(II) coordination in the different species of [Cu^{II}(Aβ3-16)] and [Cu^{II}(Aβp3-16)], the NMR data (^{1}H, ^{13}C, and 2D NMR experiments) of the corresponding peptide in the absence and presence of substoichiometric copper(II) amounts at several pH values were recorded (Figures 3 and 4 and S3−S12 in the Supporting

dx.doi.org/10.1021/ic302097d | *Inorg. Chem.* 2012, 51, 12988−13000

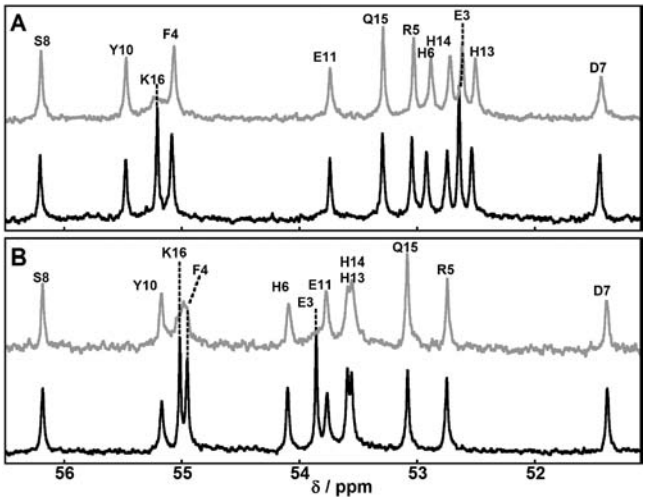

Figure 3. Cα region of the ^{13}C NMR spectrum of Aβ3-16 peptide in the absence (black) or presence (gray) of 0.02 equiv of Cu^{II} at pH 6.0 (panel A) and of 0.3 equiv of Cu^{II} at pH 8.6 (panel B). The signals affected by copper(II) addition are indicated by dotted lines. [Aβ3-16] = 10 mM, T = 25 °C, and ν = 125.8 MHz.

Information). Because copper(II) is paramagnetic and its binding to Aβ peptides is dynamic, a small stoichiometry of copper(II) will induce specific broadening of the NMR signals of residues involved in copper(II) coordination.[47] Nevertheless, because of the dynamics in solution, ^{13}C NMR can hardly distinguish the transient ligands from more stable ligands (i.e., ^{13}C NMR signals of COO^- and aromatic rings of His are both highly affected by the presence of copper(II) because they are likely involved in copper(II) exchange between peptides; see, for instance, Figures S3, S4, and S10 in the Supporting Information, panels B and F, respectively).[26] Such transient ligands may also be involved in the formation of Cu(Aβ)$_2$ species, as recently suggested by Pedersen and co-workers,[52] although in a our previous NMR study of copper binding to Aβ1-16, we found no direct evidence for the formation of such species in a significant amount.[26]

In addition to that, NMR analysis of copper(II) binding to the peptides is limited to components with less than two deprotonated amide ligands (i.e., components I, II, and II′). Indeed, copper(II) coordination involving two or more deprotonated amide groups results in a too slow copper(II) exchange and the copper(II) paramagnetic effect broadens the signal of bound peptide beyond detection. Then only the signal of a copper(II)-unbound peptide or copper(II) bound to peptide in another detectable component remains.[27,53]

Figure 3A shows the ^{13}C NMR spectrum of the Cα area of Aβ3-16 peptide in the absence and presence of 0.02% copper(II) at pH 6.0. The two signals most strongly affected belong to Lys16 and Glu3. The signal of Cα from Glu3 undergoes a large broadening, which is in line with the $-NH_2$ terminus bound to copper(II). The broadening of the Cα signal from Lys16 is attributed to binding of the free COO^- C terminus, as observed earlier for Aβ1-16.[26] However, this may not be relevant for the full-length peptide because the Aβ1-16 C terminus was not protected. Hence, the involvement of the $-NH_2$ terminal amine in copper(II) binding by the Aβ3-16 peptide is confirmed by the NMR experiments, as were previously reported for the Aβ1-16 and murine counterparts.[26,54]

In order to figure out the copper(II) coordination in component II, ^{13}C NMR was performed at higher pH. There is no pH where component II is exclusively present. Thus, pH 8.6 was chosen because only components II and III are present, but component III cannot be detected by ^{13}C NMR, in line with the presence of two deprotonated amide groups in the copper(II) binding site (see above). Hence, only changes due to component II are observed. Cα from Glu3 remains largely affected, indicating that the N-terminal NH_2 stays coordinated to the copper(II) in component II. The main change between pH 6.0 and 8.6 is the broadening of Cα from Phe4, which is attributed to deprotonation of the NH group from the Glu3−Phe4 peptide bond and its coordination to copper(II). At pH 8.6, the Cα and CO from His (Figure S4 in the Supporting Information, panels A and C) are broadened by copper(II) addition, and on the Cα/Hα correlation peak (Figure S5 in the Supporting Information), His6 is preferentially affected compared to the other two His residues, in line with the CO group of His6 involved in copper(II) binding.

At both pH values, the Cδ/Hδ and Cε/Hε of the His rings are also affected (Figures S3 and S4, panel F, and S8 and S9 in the Supporting Information), indicating His involvement in copper(II) binding in both components. Thus, taking into account the EPR and CD results, the experimental data are best explained by the following equatorial coordination site of

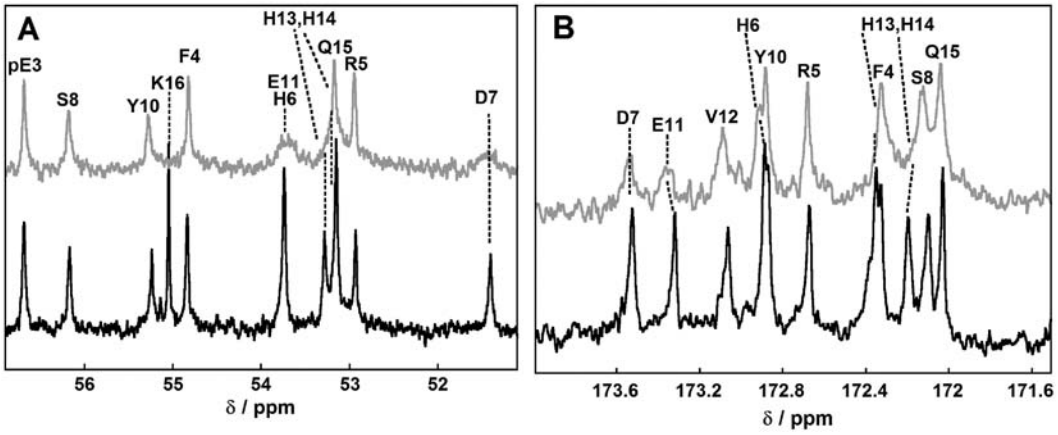

Figure 4. Cα (panel A) and CO (panel B) regions of ^{13}C NMR spectra of the Aβp3-16 peptide in the absence (black) or presence of 0.05 equiv of Cu^{II} (gray) at pH 7.0. The signals affected by copper(II) addition are indicated by dotted lines. [Aβp3-16] = 10 mM, T = 25 °C, and ν = 125.8 MHz.

dx.doi.org/10.1021/ic302097d | Inorg. Chem. 2012, 51, 12988−13000

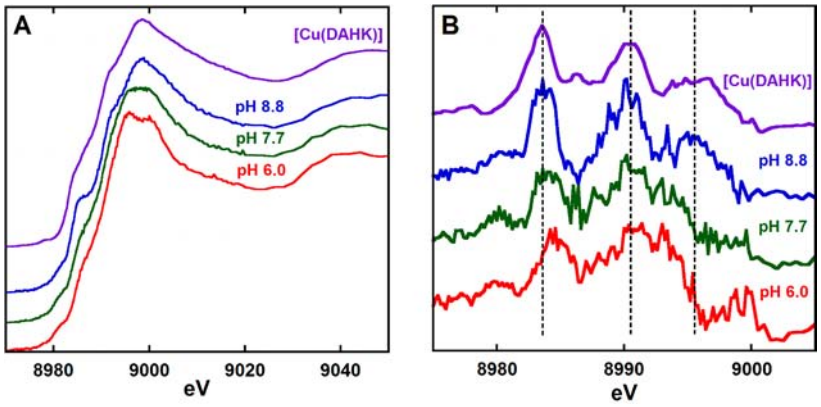

Figure 5. XANES spectra (A) and derivatives of the XANES spectra (B) of [Cu(Aβ3-16)] (red, pH 6.0; green, pH 7.7; blue, pH 8.8) and [Cu(DAHK)] (purple) complexes. Conditions: [Cu(peptide)] = 2 mM in H_2O and T = 20 K, except for [Cu(DAHK)] (see ref 53 for conditions).

copper(II) when linked to the Aβ3-16 peptide: component I {NH_2; CO; 2Im (His)} and component II {NH_2; N^- (Glu3−Phe4); Im (His6); CO (His6)}. On the basis of what was proposed on the [Cu(Aβ1-16)] species,[21] the CO function in component I of [Cu(Aβ3-16)] might come from the Glu3 amino acid residue. Indeed, this will induce the formation of a stable five-coordinated metallacycle with the $-NH_2$ terminal amine. In contrast, while in component II of the [Cu(Aβ1-16)] complex, the Glu3 CO group adjacent to the Asp1−Ala2 deprotonated amide was proposed to be involved in copper(II) binding,[22,26] in the case of [Cu(Aβ3-16)], the CO group is proposed to be that of His6 based on its selective broadening detected by NMR. It has to be noted that, based only on the size of the metallacycle formed, the {Im (His6), CO (His6)} binding is less favorable than that of {N^- (Phe4), CO (Arg5)}. Thus, the binding of CO (His6) instead of CO (Arg5) may be linked to the peculiar nature of the Arg5 side chain (bulky and charged).

In Figure 4, the two panels display the ^{13}C NMR spectra of Aβp3-16 at pH 7.0 with (gray) and without (black) copper(II) with focus on the CO (left) and Cα (right) areas. Attempts to record the NMR data at higher pH were unfruitful because broadening was not specific enough, in line with copper(II) bound by two or more deprotonated amide groups in components III′ and IV′. In contrast to component II of [Cu(Aβ3-16)] (Figure 3B, bottom), Phe4 is not affected in the case of the Aβp3-16 peptide, in line with copper(II) coordination to the N-term part (including the deprotonated amide of the Glu3−Phe4 bond) that is precluded by the presence of the pyroglutamate cycle. As a general trend, peaks from the His residues are strongly affected by added copper(II) (Figures S10−S12 in the Supporting Information), as exemplified by Cα and CO (Figure 4). In general, His13 and His14 are more affected than His6. As in component II′, there is one deprotonated amide group bound to the copper(II) center (see above); this might be explained by the preferential involvement of the deprotonated amide from the His13−His14 peptide bond rather than the His6−Asp7 bond, with the involvement of the deprotonated amide group from Arg5−His6 being discarded on the basis of previous results on copper(II) binding to Aβ1-16 and R5G-Aβ1-16.[26,54] Such a His13−N^-−His14 tripodal copper(II) binding has also been proposed using theoretical calculations[55,56] and is in line with potentiometric studies of copper(II) binding to Ac-Y10A-Aβ8-16 peptides.[57] Cα and CO from Asp7 and Glu11 are also affected by copper(II). Nevertheless, it seems that such a broadening is due to COO^- coordination to copper(II) because the side chain is more strongly affected than the backbone carbon and hydrogen atoms. This indicates a possible implication of Asp7 and Glu11 in copper(II) binding via COO^-. As was previously observed, Cα from Lys16 is affected because of COO^- binding. According to results obtained by other techniques, the most likely ligands of copper(II) in component II′ of [Cu(Aβp3-16)] are {N^- (His13−His14); Im (His13); Im (His14); Im (His6) or COO^- (Asp7, Glu11)}.

XANES Study of [Cu^{II}(Aβ3-16)] and [Cu^{II}(Aβp3-16)]. XANES spectra were recorded for [Cu(Aβ3-16)] and [Cu(Aβp3-16)] species at selected pH values (Figures 5 and S13 in the Supporting Information). In line with previous measurements by CD, EPR, and NMR, pH-dependent spectral modifications were observed because of copper(II) coordination changes with the pH for both complexes. More particularly, in the case of [Cu(Aβ3-16)], component III can be predominantly detected at pH 8.8, a situation that was not encountered for the [Cu(Aβ1-16)] species studied in the past.[27] The XANES signature of component III was compared to that of the well-described [Cu(DAHK)] peptide, where DAHK represents the N-terminal sequence of the human serum albumin.[53] In this latter species, the copper(II) site is made of the N-terminal amine, the side chain of the His residues, and the two deprotonated amides in between,[53,58] and such copper(II) coordination is predominant over a wide pH range.[59] It is worth noting that the XANES spectrum of [Cu(Aβ3-16)] at pH 8.8 (component III) and its derivative (parts A and B in Figure 5, respectively) are similar to those reported for [Cu(DAHK)] at pH 7.4.[53] This supports a similar type of first coordination sphere for copper(II) in [Cu(Aβ3-16)], i.e., the $-NH_2$, two N^-, and one imidazole ring of His, in line with the studies described above.

^{1}H NMR Study of [Cu^I(Aβ3-16)] and [Cu^I(Aβp3-16)]. To complete the structural data on copper binding to the N-terminally truncated Aβ peptides, we have performed ^1H NMR studies of [Cu^I(Aβ3-16)] and [Cu^I(Aβp3-16)] species. In Figure 6, ^1H NMR spectra of the Aβ3-16 and Aβp3-16 peptides in the presence of 0.9 equiv of Cu^I are compared to that obtained in the case of the reference Aβ1-16 peptide.[29] Similar effects of copper(I) addition on the apopeptide signature are observed for the three peptides, i.e., a shift of the two aromatic protons from the three His. In the case of Hε (see the Supporting Information for nomenclature details), a downshift

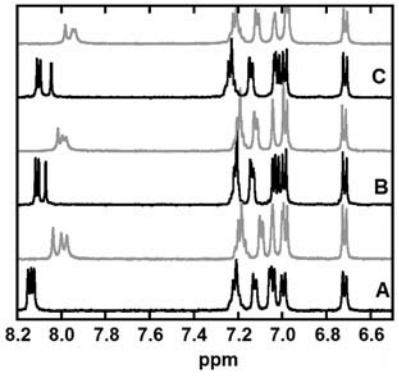

Figure 6. ^{1}H NMR spectra of Aβ1-16 (A), Aβ3-16 (B), and Aβp3-16 (C) peptides (black) and in the presence of 0.9 equiv of Cu^I (gray) in a phosphate buffer of 0.2 M and pH 6.7. [peptide] = 1 mM.

is observed that is more important for two of the three His signals (Figure 6). Concomitantly, those latter signals are more broadened. In the case of Hδ, the changes observed are more subtle and more difficult to analyze.[29] In addition to modifications on the aromatic domain, some changes are also observed in the aliphatic region for the three peptides (Figure S14 in the Supporting Information) mainly involving Gly9 to Val12 residues, modifications that can be attributed in the case of the Aβ1-16 peptide to the folding imposed by copper(I) coordination to the His13−His14 dyad.[30] Copper(I) coordination to Aβ1-16 was proposed to be dynamic including different species in equilibrium.[29] The major form was copper(I) binding to His13 and His14 (His13−Cu^I−His14) in a linear fashion.[16,28] This form was in equilibrium with two minor forms, i.e., His6−Cu^I−His13 and His6−Cu^I−His14. The shifts and broadening of the NMR signals due to copper(I) addition to either Aβ3-16 or Aβp3-16 peptide are highly similar to what was observed for Aβ1-16, strongly indicating that the copper(I) coordination site is the same in the three peptides. Thus, truncation or pyroglutamate formation at the N-terminus does not affect copper(I) binding. This confirms that the N-terminal amine is not involved in copper(I) binding.

Affinity Measurements on [Cu^{II}(Aβ3-16)] and [Cu^{II}(Aβp3-16)]. In addition to structural insight, affinity for copper(II) and copper(I) is an important parameter to evaluate because it determines whether Aβ peptide is able to bind copper ions in a biological environment, in the presence of competitive ligands.

In order to evaluate the affinities of copper(II) for the Aβ3-16 and Aβp3-16 and the Aβ1-16 and Ac-Aβ1-16 counterparts, competition experiments with a well-known copper(II) chelator, i.e., glycine amino acid, have been performed and followed by CD (Figure 7). The CD data were reproduced by considering the formation of a 1:1 Cu−peptide complex, leading to determination of the apparent affinity constant as a function of the Gly concentration. Then, the conditional affinity is deduced from the following equation, where the conditional affinity value is the affinity at a given (pH, T) couple.

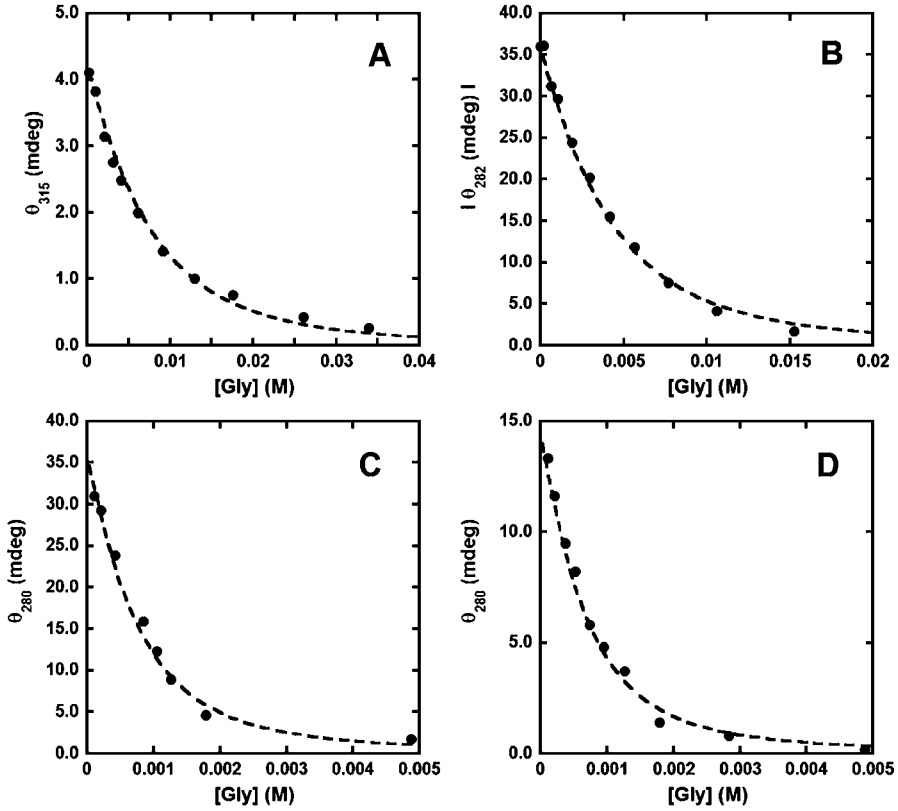

Figure 7. Gly-induced decrease of a [Cu(peptide)] LMCT band in CD spectra, together with the corresponding calculated curve: (A) [Cu(Aβ1-16)], λ = 315 nm; (B) [Cu(Aβ3-16)], λ = 282 nm; (C) [Cu(Ac-Aβ)], λ = 280 nm; (D) [Cu(Aβ1-16)], λ = 280 nm. [Cu(peptide)] = 0.5 mM, [HEPES] = 100 mM, and pH 7.4.

dx.doi.org/10.1021/ic302097d | *Inorg. Chem.* 2012, 51, 12988−13000

$$ {}^{\mathrm{cond}}K^{\mathrm{A}\beta} = {}^{\mathrm{app}}K^{\mathrm{A}\beta}\left(1 + \frac{[\mathrm{Gly}]_0}{K_{\mathrm{d}_1}^{\mathrm{Gly}}}\frac{1}{1 + 10^{-\mathrm{pH}+\mathrm{p}K_{\mathrm{a}}^{\mathrm{Gly}}}} + \frac{[\mathrm{Gly}]_0^{\,2}}{K_{\mathrm{d}_1}^{\mathrm{Gly}}K_{\mathrm{d}_2}^{\mathrm{Gly}}}\frac{1}{(1 + 10^{-\mathrm{pH}+\mathrm{p}K_{\mathrm{a}}^{\mathrm{Gly}}})^2} + \frac{[\mathrm{HEPES}]_0}{K_{\mathrm{d}}^{\mathrm{HEPES}}(1 + 10^{-\mathrm{pH}+\mathrm{p}K_{\mathrm{a}}^{\mathrm{HEPES}}})}\right) $$

$$ \mathrm{p}K_{\mathrm{a}}^{\mathrm{HEPES}} = 7.41, \quad K_{\mathrm{d}}^{\mathrm{HEPES}} = 10^{-3.22}; $$

$$ \mathrm{p}K_{\mathrm{a}}^{\mathrm{Gly}} = 9.53, \quad K_{\mathrm{d}_1}^{\mathrm{Gly}} = 10^{-8.2}, \quad K_{\mathrm{d}_2}^{\mathrm{Gly}} = 10^{-6.9} $$

Competition with the HEPES buffer has also been included but is negligible compared to competition with Gly, except for very low Gly concentration. HEPES data are from ref 60; Gly data are from the NIST database and ref 61.

Values thus obtained are reported in Table 2 and, for the Aβ1-16 peptide, are in line with most recent values reported in the literature.[18,48] Aβp3-16 and Ac-Aβ peptides have very similar affinities for the copper(II) ion, indicating that the way that the free N-terminal is blocked has only a minor impact on copper(II) coordination. In contrast, the affinity of the Aβ3-16 peptide is about 3 times weaker than that of the Aβ1-16 peptide. These relative affinity values have also been obtained by competition between Aβ1-16 and Aβ3-16 or Aβp3-16, followed by CD and fluorescence (see the Supporting Information). Acetylation or pyroglutamate formation on the N-terminal amine leads to a decrease in the affinity by 2 orders of magnitude, in line with the previous data obtained by calorimetric titration.[48,62]

Table 2. Conditional Affinity Constants of [Cu^{II}(peptide)] and [Cu^{I}(peptide)] Species (0.1 M HEPES, pH 7.4) and Corresponding Standard Deviation Constants

peptide	copper(II) affinity ($\times 10^{10}$ M^{-1})	copper(I) affinity ($\times 10^{6}$ M^{-1})	ref
Aβ1-16	1.1 ± 0.1	7.5 ± 1.0	63
Aβ3-16	0.33 ± 0.02	9.2 ± 0.9	
Aβp3-16	0.008 ± 0.001	6.5 ± 0.5	
Ac-Aβ1-16	0.01 ± 0.001	12 ± 1.3	63

Affinity Measurements on [Cu^{I}(Aβ3-16)] and [Cu^{I}(Aβp3-16)]. In a recent study of copper(I) binding to Aβ1-16, we have established that ferrozine is a copper(I) chromophore of moderate affinity and is thus suitable for competition experiments with Aβ peptides.[63] The copper(I) affinities of Aβ3-16 and Aβp3-16 peptides determined using this method are given in Table 2 and compared to those of Aβ1-16 and Ac-Aβ1-16 peptides. These four values are very close, indicating that the copper(I) site is maintained in the different peptides in line with the data obtained by NMR and the involvement of His residues only.

DISCUSSION

Copper(I) Coordination to N-Terminally Modified Aβ Peptides. Regarding copper(I) coordination to the Aβ1-16, Ac-Aβ1-16, Aβ3-16, and Aβp3-16 peptides, no significant structural and thermodynamic change is observed between the peptides in line with the involvement of only His side chains in copper(I) binding that are conserved in the four peptides.

Copper(II) Coordination to N-Terminally Truncated Aβ Peptides. The proposed copper(II) binding to the Aβ3-16 peptide as a function of the pH is described in Scheme 1A. It is worth noting that, as previously described in the case of [Cu(Aβ1-16)], several species are in equilibrium at a given pH value[26] and consequently only the main form is drawn in Scheme 1. The involvement of the $-NH_2$ terminal of Aβ3-16 is supported by the ^{13}C NMR data in both components I and II, where a strong paramagnetic relaxation enhancement effect is observed for the signals of the Aβ3-16 N-terminal region. On the basis of previous data on [Cu(Aβ1-16)] and on the data obtained here, equatorial copper(II) coordination is completed by the CO group from the Glu3−Phe4 bond and the side chain of two His residues in component I. In component II, a strong broadening effect on Phe4 Cα was detected in line with binding of the amidyl from the Glu3−Phe4 peptide bond. Also, coordination of the CO from the His6−Asp7 bond occurs

Scheme 1. Proposed [Cu(Aβ3-16)] (A) and [Cu(Aβp3-16)] (B) Complexes as a Function of pH

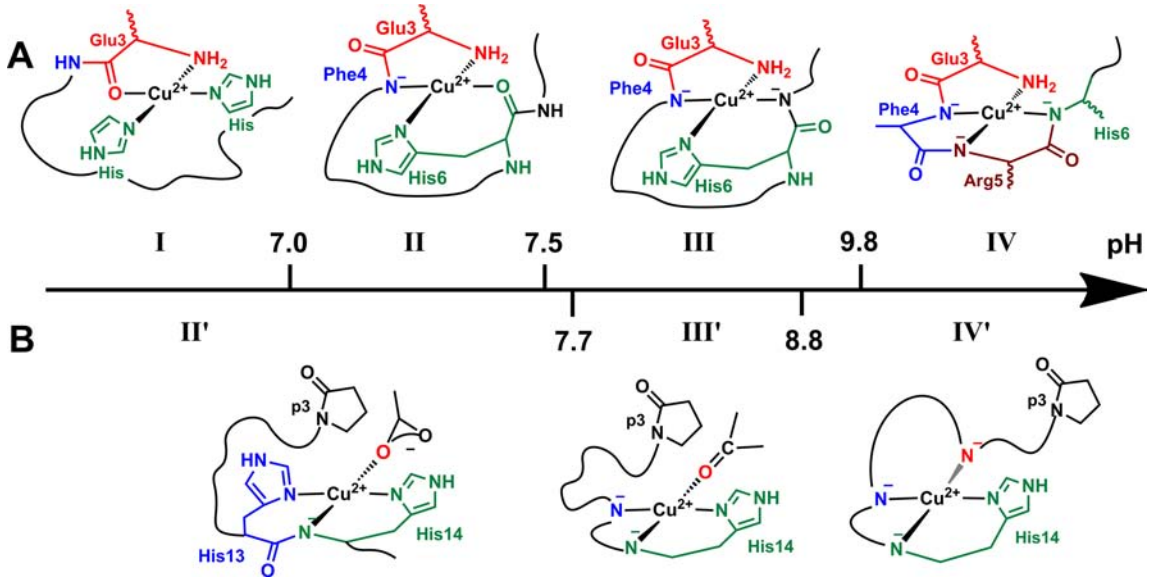

dx.doi.org/10.1021/ic302097d | Inorg. Chem. 2012, 51, 12988−13000

concomitant with decoordination of the second His side chain. This was mainly proposed on the basis of different spectral CD signatures compared to the parent [Cu(Aβ1-16)] complex ruling out the formation of two adjacent metallacycles, as in the [Cu(Aβ1-16)] case. Such CO (His 6) binding is likely unfavored on a thermodynamic point of view and may explain why component II evolves toward component III with a very low pK_a value compared to other Aβ mutants and is thus very minor in solution. In component III, the {$-NH_2$, $2N^-$, and His} binding set is deduced from the CD, EPR, and XANES measurements, and thus deprotonation of the peptide bond His6−Asp7 is proposed. The presence of two distant metallacycles is proposed from the positions of the CD, $-NH_2$-to-copper(II) and N^--to-copper(II) LMCT bands that are different compared to those of the [Cu(Aβ1-16)] complex, where two adjacent metallacycles were observed. Hence, components II and III are slightly different between [Cu(Aβ1-16)] and [Cu(Aβ3-16)]. Indeed, in the former case, two adjacent metallacycles were proposed between $-NH_2$(Asp1)−Cu^{II}−N^-(Asp1−Ala2) and N^-(Asp1−Ala2)−Cu^{II}−CO(Ala2−Glu3) (component II) or N^-(Asp1−Ala2)−Cu^{II}−N^-(Ala2−Glu3) (component III), while in the latter case, two remote metallacycles are proposed between $-NH_2$(Glu3)−Cu^{II}−N^-(Glu3−Phe4) and Im(His6)−Cu^{II}−CO(His6−Asp7) (component II) or Im(His6)−Cu^{II}−N^-(His6−Asp7) (component III). Such a trend is quite unusual because, in general, the formation of metallacycles centered on two different (N-term and His) sites is disfavored compared to the formation of several metallacycles centered on either the N-term or the side chain of His residues,[57] with the best anchoring site being strongly dependent on the peptide sequence and distance between the N-term and His.[64−66] Such a difference might originate from the presence of Arg5 that precludes the formation of the second adjacent metallacycle in the present case (see below). In component IV, the copper(II) site is strongly reshuffled, leading to a copper(II) bound to the N-terminal amine and the three adjacent deprotonated amide groups, as observed in the case of the [Cu(Aβ1-16)] complex, in line with a shift of the position of the LMCT bands in CD toward the position observed in [Cu(Aβ1-16)] for three adjacent metallacycles. Decoordination of the anchoring His at high pH may be the driving force of such a reorganization. Such His decoordination in favor of a third amide coordination at high pH is reminiscent of what was previously reported for other His-containing peptides, when the His residues lies in the fourth position or beyond from the N-terminal anchoring site (reviewed in ref 67). This is particularly true for the simplest GGGH peptide[68] and the Aβ one.[27]

Copper(II) Coordination to Pyroglutamate Forms of Aβ Peptides. For copper(II) binding to the Aβp3-16 peptides, as expected from preclusion of the NH_2 terminal binding, His act(s) as anchoring residues for copper(II) (Scheme 1B). In component II′, all of the available data converge toward a copper(II) binding site made by two imidazole rings from His, a deprotonated amidyl function, and either a carboxylate function or an imidazole ring from the third His residue, where the former proposition is favored based on the drastic broadening observed by NMR on the Asp7 and Glu11 side chains. In component III′, detected at higher pH, EPR data are in line with deprotonation of a second amidyl function, leading to a copper(II) binding site made by one (anchoring) imidazole ring from His, two deprotonated amidyl functions, and a carbonyle or a carboxylate function or an imidazole ring from a second His residue. On the basis of the similarity of the EPR data reporting copper(II) binding to the Ac-GGGTH-NH_2 peptide in component III′,[69] in which the copper(II) site was one imidazole ring from His, two deprotonated amidyl functions, and a carbonyle function, the former possibility is favored. In component IV′, a third amidyl function replaces the carbonyl one, leading to a {His, $3N^-$} copper(II) binding site.

Copper(II) Coordination to N-Terminally Modified Aβ Peptides: First-Coordination-Sphere Effects. The results obtained here by multiple complementary techniques (NMR, CD, XANES, and EPR) on copper(I) and copper(II) binding to Aβ3-16 and Aβp3-16 agree in terms of the nature of the different components observed as a function of the pH. According to these results, pH-dependent copper(II) coordination models are proposed in Scheme 1. For copper(II), the N-terminal amine plays a crucial role in line with its participation in copper(II) anchoring. Indeed, the absence of the free N-terminal amine reduces the copper(II) affinity, and the copper(II) site is located around the His residues only. This is the reason why the spectroscopic features of [Cu(Aβ3-16)] compare well with [Cu(Aβ1-16)], on the one hand, and [Cu(Aβp3-16)] with [Cu(Ac-Aβ1-16)], on the other hand. The two major CD differences between the two peptide groups is the shape of d−d and $-NH_2$ LMCT bands. The same distinction can be made regarding the EPR data obtained as a function of the pH. However, the EPR results alone can be misleading, especially in the absence of the attribution of all components as a function of the pH. This was the case for Drew et al.,[43] who concluded that copper(II) binds to Aβ3-16 and Aβp3-16 peptides in a similar way because of similar EPR parameters. They only detected the EPR signatures of two components for both Aβ3-16 and Aβp3-16 peptides, a "low-pH" component predominant at pH 6.3 (Aβ3-16) and pH 6.9 (Aβp3-16), and a "high-pH" component predominant at pH 8.5 (Aβ3-16) and above pH 9 (Aβp3-16).[43] Including their EPR data in Table 1 clearly shows that for the [Cu(Aβ3-16)] complex their "low-pH" component corresponds to component I and their "high-pH" form to component III. This is in line with a component II that never predominates in solution and is thus difficult to detect properly. Similarly, for the [Cu(Aβp3-16)] species, their "low-pH" form corresponds to component II′ and their "high-pH" form to component IV′. As can be seen in Table 1, components I and II′, on the one hand, and III and IV′, on the other hand, have comparable EPR parameters, hence the ill-interpretation of the EPR data in ref 43. Thus, the full component assignments over a large pH range and the use of complementary methods such as CD and NMR are crucial to correctly assign the components because the same EPR parameters do not imply the same copper(II) coordination sphere.

Copper(II) affinities for the different peptide studied here are in line with the coordination site proposed based on spectroscopic data. Indeed, copper(II) binding to the N-terminal amine of Aβ3-16 (and Aβ1-16) is also in agreement with the significant drop of the copper(II) affinity due to free N-terminal amine blocked in the case of Ac-Aβ1-16 and Aβp3-16 peptides. It is also worth noting that the copper(II) affinity for Aβ3-16 is slightly weaker than that for the Aβ1-16 peptide, while copper(II) coordination to the two peptides at pH 7.4 is different. Indeed, at pH 7.4, the main component in [Cu(Aβ1-16)] is I, including one metallacycle, whereas the main component in [Cu(Aβ3-16)] is II, including two metallacycles. Thus, the affinity measurements indicate that the formation of a

dx.doi.org/10.1021/ic302097d | Inorg. Chem. 2012, 51, 12988−13000

Scheme 2. Proposed Interaction To Rationalize the Different Species pK_a(I/II) Values Determined between the [Cu(peptide)] Complexes[a]

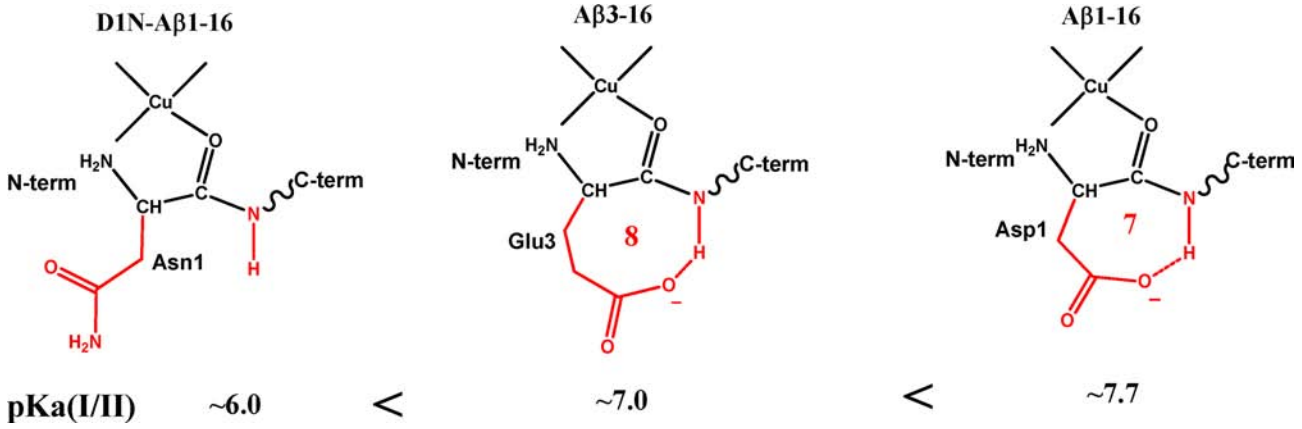

[a]In red, the N−H that undergoes deprotonation in component II (upper scheme) and the residue proposed to be involved with it.

second metallacyle is not favorable in terms of the copper(II) affinity. Such a similar trend has been recently observed for Cu(peptide) model systems encompassing two or three metallacycles.[70]

Copper(II) Coordination to N-Terminally Modified Aβ Peptides: Effects beyond the First Coordination Sphere. The four complexes [Cu(Aβ1-16)], [Cu(Aβ3-16)], [Cu(Ac-Aβ1-16)], and [Cu(Aβp3-16)] successively switch from component I/I′ to IV/IV′ via an additional amidyl binding for each further species. However, the pK_a values between two successive components are significantly different in the case of the [Cu(Aβ1-16)] and [Cu(Aβ3-16)] complexes (Table 1), while they are close in the case of [Cu(Ac-Aβ1-16)] and [Cu(Aβp3-16)]. In the latter case, this could be explained by the fact that a free N-terminal is not available for copper(II) coordination, leading to the same set of ligands for both Aβp3-16 and AcAβ. In contrast, the high variation in the pK_a(I/II) values between the [Cu(Aβ1-16)] and [Cu(Aβ3-16)] complexes can be rationalized by second-sphere effects (Scheme 2) in line with the pK_a(I/II) value previously determined for the mutants D1N.[27,71] The key step between component I/II is deprotonation of the NH amide backbone. If the −NH function is stabilized by its involvement in intramolecular interaction such as hydrogen bonding, then the pK_a value between two successive components will be higher. This is typically the case for pK_a(I/II) values within the series of [Cu(D1N-Aβ1-16)], [Cu(Aβ3-16)], and [Cu(Aβ1-16)] species in which pK_a(I/II) is ~6.0,[27,71] ~7.0, and ~7.7, respectively. The highest stabilization of component I is observed for the [Cu(Aβ1-16)] complex, where the NH is stabilized by the hydrogen bond from COO^- of Asp1 forming a seven-membered ring. In [Cu(Aβ3-16)], a more moderate stabilization occurs because of the formation of an eight-membered metallacycle (compared to seven-membered). No stabilization is detected in [Cu(D1N-Aβ1-16)] because the lone pair NH_2 of Asn1 is mainly delocalized on the adjacent carbonyl and can thus not be involved in hydrogen-bond interaction.

The Arg5 residue, while not directly involved in copper(II) coordination, seems to play a crucial role in copper(II) binding to [Cu(Aβ3-16)] by precluding the formation of a second metallacycle adjacent to the first $-NH_2-Cu^{II}-N^-$ cycle, in contrast to what was previously observed in the case of [Cu(Aβ1-16)]. Similar Arg5 effects were observed in the comparative study of copper(II) binding to the human and to its R5G mutant because replacement of Arg5 by Gly induces deprotonation of the Gly5−His6 peptide bond instead of the Asp1−Ala2 bond in the Aβ1-16 case.[54] Also, Arg indirect effects, i.e., effects not related to binding of the side chain of Arg to Cu, were encountered in other studies. For instance, the copper(II) binding site of angiotensin II (sequence DRVYIH), initially observed around His6, moves to the N-term part with deprotonation of the Asp1−Arg2 and Arg2−Val3 bonds at high pH.[72] This is reminiscent of what was observed here between components III and IV, where the metal center site has been reshuffled at high pH with deprotonation of the Phe4−Arg5 and Arg5−His6 bonds. Also, in sequence with specific nickel(II) peptide bond hydrolysis, Arg was shown to increase particularly the hydrolytic activity compared to other amino acids.[65] In the present case, the exact origin of such an Arg5 effect needs further investigation to be correctly depicted.

CONCLUDING REMARKS

The present study has revealed the copper(I) and copper(II) binding spheres to the two biologically relevant truncated forms of the Alzheimer peptide Aβ, i.e., Aβ3-16 and Aβp3-16. The application of a multispectroscopic approach (NMR, EPR, CD, and XANES) including affinity studies was crucial to deciphering the different components of the [Cu(peptide)] complexes and to identifying the most likely ligands in the components present at pH close to the physiological value. It turned out that, when available, the free N-terminal amine is the main anchor for copper(II) binding, as observed in the [Cu(Aβ1-16)] and [Cu(Aβ3-16)] complexes. When the N-terminal amine is blocked, as observed in the [Cu(Ac-Aβ1-16)] and [Cu(Aβp3-16)] complexes, His will take over the anchoring role. In addition to that feature, the present data also reveal an important role of the second-sphere environment because pH-dependent copper(II) coordination to Aβ1-16 and Aβ3-16 is significantly different. Hence, at physiological pH, the main coordination sites are altered in Aβ3-16 compared to Aβ1-16, with component I or II being predominant in the latter or former case, respectively. This also implies that Aβ modification of residues not directly involved in copper(II) binding does change the copper(II) binding site and can thus impact the aggregation and ROS production properties of the [Cu-

(peptide)] complexes. Such a scenario might be of particular interest in the case of familial AD in which Aβ mutations have been reported. A well-known copper(II) coordination chemistry to these important N-terminally modified Aβ forms is a prerequisite for further studies on aggregation and toxicity. Such studies are currently in progress in our group.

■ ASSOCIATED CONTENT

Supporting Information

pH-dependent EPR, NMR, and XANES spectra of [Cu^{II}(peptide] complexes, assignments of the ^{1}H and ^{13}C NMR signals of the Aβ3-16 and Aβp3-16 peptides, NMR spectra of [Cu^{I}(peptide] complexes, and CD and Tyr10 fluorescence competition experiments. This material is available free of charge via the Internet at http://pubs.acs.org.

■ AUTHOR INFORMATION

Corresponding Author

*E-mail: bruno.alies@lcc-toulouse.fr (B.A.), christelle.hureau@lcc-toulouse.fr (C.H.). Tel.: (+33) 5 61 33 31 62. Fax: (+33) 5 61 55 30 03.

Notes

The authors declare no competing financial interest.

■ ACKNOWLEDGMENTS

Financial support from ANR NEUROMETALS (Agence Nationale de la Recherche; Grant Neurometals NT09-488591) as well as SOLEIL for the provision of synchrotron radiation on the SAMBA beamline (Proposal 20110116) is acknowledged. E. Renaglia is ackowledged for recording of the Tyr10 fluorescence data.

■ REFERENCES

(1) Puzzo, D.; Arancio, O. *J. Alzheimer's Dis.* **2012**, DOI: 10.3233/JAD-2012-129033.
(2) Holtzman, D. M.; Morris, J. C.; Goate, A. M. *Sci. Transl. Med.* **2011**, *3*, 77sr1.
(3) Hardy, J.; Selkoe, D. J. *Science* **2002**, *297*, 353−356.
(4) Klein, W. L.; Stine, W. B., Jr.; Teplow, D. B. *Neurobiol. Aging* **2004**, *25*, 569−580.
(5) Haass, C.; Selkoe, D. J. *Nat. Rev. Cell. Mol. Biol.* **2007**, *8*, 101−112.
(6) Gadad, B. S.; Britton, G. B.; Rao, K. S. *J. Alzheimer's Dis.* **2011**, *24*, 223−232.
(7) Ono, K.; Yamada, M. *J. Neurochem.* **2011**, *117*, 19−28.
(8) Lovell, M. A.; Robertson, J. D.; Teesdale, W. J.; Campbell, J. L.; Markesbery, W. R. *J. Neurol. Sci.* **1998**, *158*, 47−52.
(9) Miller, L. M.; Wang, Q.; Telivala, T. P.; Smith, R. J.; Lanzirotti, A.; Miklossy, J. *J. Struct. Biol.* **2006**, *155*, 30−37.
(10) Roychaudhuri, R.; Yang, M.; Hoshi, M. M.; Teplow, D. B. *J. Biol. Chem.* **2009**, *284*, 4749−4753.
(11) Donnelly, P. S.; Xiao, Z.; Wedd, A. G. *Curr. Opin. Chem. Biol.* **2007**, *11*, 128−133.
(12) Adlard, P. A.; Bush, A. I. *J. Alzheimer's Dis.* **2006**, *10*, 145−163.
(13) Karr, J. W.; Kaupp, L. J.; Szalai, V. A. *J. Am. Chem. Soc.* **2004**, *126*, 13534−13538.
(14) Minicozzi, V.; Stellato, F.; Comai, M.; Dalla Serra, M.; Potrich, C.; Meyer-Klaucke, W.; Morante, S. *J. Biol. Chem.* **2008**, *283*, 10784−10792.
(15) Syme, C. D.; Nadal, R. C.; Rigby, S. E.; Viles, J. H. *J. Biol. Chem.* **2004**, *279*, 18169−18177.
(16) Shearer, J.; Szalai, V. A. *J. Am. Chem. Soc.* **2008**, *130*, 17826−17835.
(17) Faller, P.; Hureau, C. *Dalton Trans.* **2009**, 1080−1094.
(18) Sarell, C. J.; Syme, C. D.; Rigby, S. E.; Viles, J. H. *Biochemistry* **2009**, *48*, 4388−4402.
(19) Zawisza, I.; Rózga, M.; Bal, W. *Coord. Chem. Rev.* **2012**, *256*, 2297−2307.
(20) Hureau, C. *Coord. Chem. Rev.* **2012**, *256*, 2164−2174.
(21) Hureau, C.; Dorlet, P. *Coord. Chem. Rev.* **2012**, *256*, 2175−2187.
(22) Dorlet, P.; Gambarelli, S.; Faller, P.; Hureau, C. *Angew. Chem., Int. Ed.* **2009**, *48*, 9273−9276.
(23) Drew, S. C.; Masters, C. L.; Barnham, K. J. *J. Am. Chem. Soc.* **2009**, *131*, 8760−8761.
(24) Drew, S. C.; Noble, C. J.; Masters, C. L.; Hanson, G. R.; Barnham, K. J. *J. Am. Chem. Soc.* **2009**, *131*, 1195−1207.
(25) Kowalik-Jankowska, T.; Ruta, M.; Wisniewska, K.; Lankiewicz, L. *J. Inorg. Biochem.* **2003**, *95*, 270−282.
(26) Hureau, C.; Coppel, Y.; Dorlet, P.; Solari, P. L.; Sayen, S.; Guillon, E.; Sabater, L.; Faller, P. *Angew. Chem., Int. Ed.* **2009**, *48*, 9522−9525.
(27) Alies, B.; Eury, H.; Bijani, C.; Rechignat, L.; Faller, P.; Hureau, C. *Inorg. Chem.* **2011**, *50*, 11192−11201.
(28) Himes, R. A.; Park, G. Y.; Siluvai, G. S.; Blackburn, N. J.; Karlin, K. D. *Angew. Chem., Int. Ed.* **2008**, *47*, 9084−9087.
(29) Hureau, C.; Balland, V.; Coppel, Y.; Solari, P. L.; Fonda, E.; Faller, P. *J. Biol. Inorg. Chem.* **2009**, 995−1000.
(30) Furlan, S.; Hureau, C.; Faller, P.; La Penna, G. *J. Phys. Chem. B* **2010**, *114*, 15119−15133.
(31) Harigaya, Y.; Saido, T. C.; Eckman, C. B.; Prada, C. M.; Shoji, M.; Younkin, S. G. *Biochem. Biophys. Res. Commun.* **2000**, *276*, 422−427.
(32) Jawhar, S.; Wirths, O.; Bayer, T. A. *J. Biol. Chem.* **2011**, *286*, 38825−38832.
(33) Wirths, O.; Breyhan, H.; Cynis, H.; Schilling, S.; Demuth, H. U.; Bayer, T. A. *Acta Neuropathol. (Berlin)* **2009**, *118*, 487−496.
(34) Schlenzig, D.; Rönicke, R.; Cynis, H.; Ludwig, H. H.; Scheel, E.; Reymann, K.; Saido, T.; Hause, G.; Schilling, S.; Demuth, H. U. *J. Neurochem.* **2012**, *121*, 774−784.
(35) Schilling, S.; Zeitschel, U.; Hoffmann, T.; Heiser, U.; Francke, M.; Kehlen, A.; Holzer, M.; Hutter-Paier, B.; Prokesch, M.; Windisch, M.; Jagla, W.; Schlenzig, D.; Lindner, C.; Rudolph, T.; Reuter, G.; Cynis, H.; Montag, D.; Demuth, H. U.; Rossner, S. *Nat. Med.* **2008**, *14*, 1106−1111.
(36) Frost, J. L.; Liu, B.; Kleinschmidt, M.; Schilling, S.; Demuth, H. U.; Lemere, C. A. *Neurodegener. Dis.* **2012**, *10*, 265−270.
(37) Wittnam, J. L.; Portelius, E.; Zetterberg, H.; Gustavsson, M. K.; Schilling, S.; Koch, B.; Demuth, H. U.; Blennow, K.; Wirths, O.; Bayer, T. A. *J. Biol. Chem.* **2012**, *287*, 8154−8162.
(38) Güntert, A.; Döbeli, H.; Bohrmann, B. *Neuroscience* **2006**, *143*, 461−475.
(39) Wirths, O.; Bethge, T.; Marcello, A.; Harmeier, A.; Jawhar, S.; Lucassen, P. J.; Multhaup, G.; Brody, D. L.; Esparza, T.; Ingelsson, M.; Kalimo, H.; Lannfelt, L.; Bayer, T. A. *J. Neural Transm.* **2010**, *117*, 85−96.
(40) Schlenzig, D.; Manhart, S.; Cinar, Y.; Kleinschmidt, M.; Hause, G.; Willbold, D.; Funke, S. A.; Schilling, S.; Demuth, H. U. *Biochemistry* **2009**, *48*, 7072−7078.
(41) Schilling, S.; Lauber, T.; Schaupp, M.; Manhart, S.; Scheel, E.; Böhm, G.; Demuth, H. U. *Biochemistry* **2006**, *45*, 12393−12399.
(42) Nussbaum, J. M.; Schilling, S.; Cynis, H.; Silva, A.; Swanson, E.; Wangsanut, T.; Tayler, K.; Wiltgen, B.; Hatami, A.; Rönicke, R.; Reymann, K.; Hutter-Paier, B.; Alexandru, A.; Jagla, W.; Graubner, S.; Glabe, C. G.; Demuth, H. U.; Bloom, G. S. *Nature* **2012**, *485*, 651−655.
(43) Drew, S. C.; Masters, C. L.; Barnham, K. J. *PloS One* **2011**, *5*, e15875.
(44) Delgado, R.; Da Silva, J. J. R. F.; Amorim, M. T. S.; Cabral, M. F.; Chaves, S.; Costa, J. *Anal. Chim. Acta* **1991**, *245*, 271−282.
(45) Krezel, A.; Bal, W. *J. Inorg. Biochem.* **2004**, *98*, 161−166.
(46) Solomon, E. I. *Inorg. Chem.* **2006**, *45*, 8012−8025.
(47) Faller, P.; Hureau, C.; Dorlet, P.; Hellwig, P.; Coppel, Y.; Collin, F.; Alies, B. *Coord. Chem. Rev.* **2012**, *256*, 2381−2396.

(48) Hong, L.; Carducci, T. M.; Bush, W. D.; Dudzik, C. G.; Millhauser, G. L.; Simon, J. D. *J. Phys. Chem. B* **2010**, *114*, 11261−11271.
(49) Karr, J. W.; Akintoye, H.; Kaupp, L. J.; Szalai, V. A. *Biochemistry* **2005**, *44*, 5478−5487.
(50) Livera, C.; Pettit, L. D.; Bataille, M.; Krembel, J.; Bal, W.; Kozlowski, H. *J. Chem. Soc., Dalton Trans.* **1988**, 1357−1360.
(51) Peisach, J.; Blumberg, W. E. *Arch. Biochem. Biophys.* **1974**, *165*, 691−708.
(52) Pedersen, J. T.; Teilum, K.; Heegaard, N. H. H.; Østergaard, J.; Adolph, H.-W.; Hemmingsen, L. *Angew. Chem., Int. Ed.* **2011**, *50*, 2532−2535.
(53) Hureau, C.; Eury, H.; Guillot, R.; Bijani, C.; Sayen, S.; Solari, P. L.; Guillon, E.; Faller, P.; Dorlet, P. *Chem.—Eur. J.* **2011**, *17*, 10151−10160.
(54) Eury, H.; Bijani, C.; Faller, P.; Hureau, C. *Angew. Chem., Int. Ed.* **2011**, *50*, 901−905.
(55) Raffa, D. F.; Rickard, G. A.; Rauk, A. *J. Biol. Inorg. Chem.* **2007**, *12*, 147−164.
(56) Raffa, D. F.; Gómez-Balderas, R.; Brunelle, P.; Rickard, G. A.; Rauk, A. *J. Biol. Inorg. Chem.* **2005**, *10*, 887−902.
(57) Damante, C. A.; Osz, K.; Nagy, Z.; Pappalardo, G.; Grasso, G.; Impellizzeri, G.; Rizzarelli, E.; Sóvágó, I. *Inorg. Chem.* **2008**, *47*, 9669−9683.
(58) Harford, C.; Sarkar, B. *Acc. Chem. Res.* **1997**, *30*, 123−130.
(59) Sokolowska, M.; Krezel, A.; Dyba, M.; Szewczuk, Z.; Bal, W. *Eur. J. Biochem.* **2002**, *269*, 1323−1331.
(60) Sokołowska, M.; Bal, W. *J. Inorg. Biochem.* **2005**, *99*, 1653−1660.
(61) Kiss, T.; Sovago, I.; Gergely, A. *Pure Appl. Chem.* **1991**, *63*, 597−638.
(62) Sacco, C.; Skowronsky, R. A.; Gade, S.; Kenney, J. M.; Spuches, A. M. *J. Biol. Inorg. Chem.* **2012**, *17*, 531−541.
(63) Alies, B.; Badei, B.; Faller, P.; Hureau, C. *Chem.—Eur. J.* **2012**, *18*, 1161−1167.
(64) Bal, W.; Jezowska-Bojczuk, M.; Kozlowski, H.; Chruscinski, L.; Kupryszewski, G.; Witczuk, B. *J. Inorg. Biochem.* **1995**, *57*, 235−247.
(65) Jancsó, A.; Selmeczi, K.; Gizzi, P.; Nagy, N. V.; Gajda, T.; Henry, B. *J. Inorg. Biochem.* **2011**, *105*, 92−101.
(66) Pettit, L. D.; Pyburn, S.; Bal, W.; Kozlowski, H.; Bataille, M. *J. Chem. Soc., Dalton Trans.* **1990**, 3565−3570.
(67) Kozłowski, H.; Kowalik-Jankowska, T.; Jezowska-Bojczuk, M. *Coord. Chem. Rev.* **2005**, *249*, 2323−2334.
(68) Várnagy, K.; Szabó, J.; Sóvágó, I.; Malandrinos, G.; Nick, H.; Sanna, D.; Micera, G. *J. Chem. Soc., Dalton Trans.* **2000**, 467−472.
(69) Hureau, C.; Charlet, L.; Dorlet, P.; Gonnet, F.; Spadini, L.; Anxolabéhère-Mallart, E.; Girerd, J.-J. *J. Biol. Inorg. Chem.* **2006**, *11*, 735−744.
(70) Trapaidze, A.; Hureau, C.; Bal, W.; Winterhalter, M.; Faller, P. *J. Biol. Inorg. Chem.* **2012**, *17*, 37−47.
(71) Karr, J. W.; Szalai, V. A. *J. Am. Chem. Soc.* **2007**, *129*, 3796−3797.
(72) Decock-Le Reverend, B.; Liman, F.; Livera, C.; Pettit, L. D.; Pyburn, S.; Kozlowski, H. *J. Chem. Soc., Dalton Trans.* **1988**, 887−894.